FIBER OPTIC CHARACTERIZATION FOR UNPRECEDENTED SKY SUBTRACTION

An Undergraduate Research Scholars Thesis

by

SHRAVAN VENGALIL MENON

Submitted to the LAUNCH: Undergraduate Research office at
Texas A&M University
in partial fulfillment of the requirements for the designation as an

UNDERGRADUATE RESEARCH SCHOLAR

Approved by
Faculty Research Advisor: Dr. Jennifer L. Marshall

May 2023

Major: Physics-Astrophysics, B.S.

RESEARCH COMPLIANCE CERTIFICATION

Research activities involving the use of human subjects, vertebrate animals, and/or biohazards must be reviewed and approved by the appropriate Texas A&M University regulatory research committee (i.e., IRB, IACUC, IBC) before the activity can commence. This requirement applies to activities conducted at Texas A&M and to activities conducted at non-Texas A&M facilities or institutions. In both cases, students are responsible for working with the relevant Texas A&M research compliance program to ensure and document that all Texas A&M compliance obligations are met before the study begins.

I, Shravan Vengalil Menon, certify that all research compliance requirements related to this Undergraduate Research Scholars thesis have been addressed with my Faculty Research Advisor prior to the collection of any data used in this final thesis submission.

This project did not require approval from the Texas A&M University Research Compliance & Biosafety office.

TABLE OF CONTENTS

ABSTRACT

Fiber Optic Characterization for Unprecedented Sky Subtraction

Shravan Vengalil Menon
Department of Physics and Astronomy
Texas A&M University

Faculty Research Advisor: Dr. Jennifer L. Marshall
Department of Physics and Astronomy
Texas A&M University

Observations taken from ground-based telescopes and large spectroscopic facilities are contaminated by emission from the Earth's atmosphere and must be subtracted from astronomical measurements to recover the true target spectrum of an object. Precise and accurate sky subtraction is imperative to achieving reliable science results since many astronomical objects are fainter than the sky background. The Fiber Optic Characterization for Unprecedented Sky Subtraction (FOCUSS) project aims to obtain an accurate subtraction of the sky background using calibrated fiber-fed spectroscopic instruments for the next generation of spectroscopic facilities such as the Maunakea Spectroscopic Explorer (MSE). The fundamental basis of FOCUSS is to take detailed measurements of individual fibers that will be used in these spectroscopic facilities, locate and analyze the primary depreciators of fiber performance, and identify solutions and techniques to limit these effects. The fiber characteristics tested in the project include focal ratio degradation (FRD) and the relative transmission of the fibers. Ultimately, we should be able to choose a group of fibers for any spectroscopic facility that effectively minimize the effect of fiber differences to achieve accurate sky subtraction and maximize the accuracy of the spectroscopic data collected.

ACKNOWLEDGMENTS

Contributors

I would like to thank my faculty advisor, Dr. Jennifer L. Marshall, Dr. Luke Schmidt, and Erika Cook, for their guidance and support throughout the course of this research.

Thanks also go to my friends and colleagues and the department faculty and staff for making my time at Texas A&M University a great experience.

Finally, thanks to my family for their encouragement, patience and love.

The setup of the apparatus and the scripts used in the analyses depicted in Fiber Optic Characterization for Unprecedented Sky Subtraction were constructed in part by Silvana Delgado-Andrade, Enrique Gonzalez-Vega, Chelsea Taylor, and Lars Walker.

All other work conducted for the thesis was completed by the student independently.

Funding Sources

Undergraduate research was supported by the Munnerlyn Astronomy and Space Sciences Lab at Texas A&M University.

This work was also made possible in part by NSF under Grant Number 2009430. Its contents are solely the responsibility of the authors and do not necessarily represent the official views of the NSF.

NOMENCLATURE

FOCUSS	Fiber Optic Characterization for Unprecedented Sky Subtraction
FRD	Focal Ratio Degradation
MSE	Maunakea Spectroscopic Explorer
FWHM	Full-Width Half Max

1. INTRODUCTION

The advent of next-generation astronomical facilities in the coming decades will enable a vast array of transformative scientific studies, spanning a diverse range of subject matter. These facilities house numerous imaging surveys that have opened a new perspective on the universe by making it possible to study stars and galaxies that were previously too faint to be observed. To fully realize the scientific potential of these surveys, a significant proportion of the objects identified must be studied in more detail using spectroscopic techniques. However, given the sheer number of objects to be studied (with some individual science cases requiring observations of tens of millions of objects), it is essential that a rigorous and efficient process be developed to facilitate the execution of this science. To optimize observing time and scientific productivity, it is crucial that the spectroscopic surveys be specialized in nature, or that sufficient time is dedicated to the relevant instruments. Additionally, the capabilities of these instruments, including sensitivity, wavelength coverage, and target density, must be carefully aligned with the imaging surveys being conducted in order to maximize the overall impact of these studies.

The utilization of fiber-fed spectroscopic instruments poses a potential challenge to accuracy due to the variable transmission of individual fibers, which can be attributed to variations in material composition, strains, and stresses along the path between the light injection at the telescope focal plane and its eventual injection into a remote spectrograph as shown in [1]. Despite this challenge, established operational methods have been developed for fiber-fed multi-object spectrographs, such as the utilization of a limited number of "sky fibers" that are consistently pointed at an area of the sky without a target or the utilization of "beam-switching" to provide all fibers with sky measurements. Both of these techniques have been demonstrated to be effective to some degree [2], [3]. The measurement obtained through sky fibers is employed to create an appropriate measurement of the sky emission, which is subsequently subtracted from similar measurements of a target object or numerous target measurements. However, it must be noted that each individual

fiber in the system may possess distinct characteristics relative to the fibers designated to measure the sky contribution. The sky emission over several degrees has been acknowledged to be uniform to a degree less than 0.1% [4]. While most operational multi-fiber spectroscopic facilities are relatively unaffected by these effects, this is largely due to the fact that the objects measured by these explorers are brighter than the sky background. The science targets of numerous future projects such as the such as the Hobby-Eberly Telescope Dark Energy eXperiment (HETDEX) are fainter than the sky background, and hence would be susceptible to these effects. Additionally with the increasing use of larger and more sensitive facilities, such as PFS on Subaru, MSE, and other 10m-class fiber-fed spectrographs, as well as fiber-feeds for GMT/TMT/ELT spectrographs, it is imperative to carefully address fiber transmission to avoid limitations on data quality and science capability. As part of FOCUSS, we outline a plan to develop a suite of measurement techniques to characterize and select fiber packages. This plan will enable the achievement of unprecedentedly accurate sky subtraction levels of below 0.1%, ensuring that the science goals of many fiber-fed facilities operating at optical wavelengths are met. The proposed approach will also ensure that observations are limited only by photon noise and not systematic errors in fiber transmission. Thus, it is evident that the more uniform all fibers in a large system are in all characteristics, the more easily and accurately the sky contribution can be removed.

The measurements of key fiber characteristics that FOCUSS aims to undertake will allow for a more consistent selection of fibers for a variety of instrumentation on any telescope, as well as establish a uniform set of evaluation criteria for understanding the effects of varying conditions on critical fiber characteristics. The results of this work will yield recommendations for maximizing performance in a sky subtraction context for a broad range of facilities, including the MSE and other highly multiplexed instruments. Furthermore, the findings of this research will also be applicable to any fiber-fed instrumentation utilized for the study of extremely faint objects, making it a valuable resource for the astronomical community.

2. METHODS

This section will introduce the two key fiber characteristics primarily tested as well as other characteristics relevant to astronomical instrumentation, the research setup used to perform said tests, and techniques used to analyze them.

2.1 Focal Ratio Degradation

The Focal Ratio Degradation (FRD) of a fiber is the decrease of light's focal ratio between the input and output of an optical fiber caused by fiber optics. It is one of the major depreciators of fiber performance, and when optimized, can significantly improve the measurements obtained by any massively multiplexed spectroscopic facility.

2.1.1 Previous efforts to calculate FRD

One of the earliest studies on FRD was published by [5]. The authors developed a theoretical model for predicting the amount of FRD caused by various imperfections in a telescope's optical system. They found that FRD was primarily influenced by the scattering and absorption of light within the system, as well as any misalignments between the optical components. More recently, there have been many studies on FRD, covering a wide range of applications and optical systems. Some of these include:

Laboratory measurements have been used to study the FRD of optical fibers commonly used in astronomical spectrographs, as seen in [6]. The authors found that the FRD values varied depending on the specific fiber design and fabrication method, and they used these measurements to develop a model for predicting the FRD of similar fibers. [7] used observations of the planetary nebula NGC 7293 to measure the FRD of an optical system. The authors found that the FRD value varied with different types of optical elements and that it had a significant impact on the observed brightness distribution of the nebula. This study demonstrated the importance of measuring FRD in real-world astronomical observations. [8] developed a computer simulation to model the effects of various imperfections on the FRD of an optical system. The authors found that certain types

of aberrations, such as astigmatism and coma, had a particularly strong impact on FRD, and they proposed a method for mitigating these effects by optimizing the tilt and decenter of the optical elements. [9] conducted a study on the FRD of the Gemini South telescope, using laboratory measurements and astronomical observations of star clusters. The authors found that the FRD values fluctuated with the wavelength of light and the position on the focal plane, and they used these measurements to develop a model for predicting the FRD of the telescope. [10] developed a method for measuring FRD using a specialized pinhole camera system. The authors found that their method was able to measure FRD values with high precision and accuracy, and they used this method to study the FRD of a range of optical systems, including telescopes, camera lenses, and fibers.

Overall, these studies demonstrate the diverse range of approaches that have been used to study and measure FRD, and the importance of understanding and mitigating this effect in order to optimize image quality in a variety of applications. From the literature review above, we can definitively conclude that there are a multitude of ways to test the FRD of a fiber, and that there are pros and cons to each method.

2.1.2 FRD Setup for FOCUSS

The FRD will be measured using the method described by [11], which involves imaging the far field illumination pattern of the test fiber with a camera mounted to a translation stage which is stepped by a known amount. Light is passed through the fiber via a fiber injection system, and all aspects of the test are controlled by a python script. The hardware involved will be controlled using the corresponding application programming interface for each component. The schematic of the testing apparatus used is shown below in **Figure 1** [12].

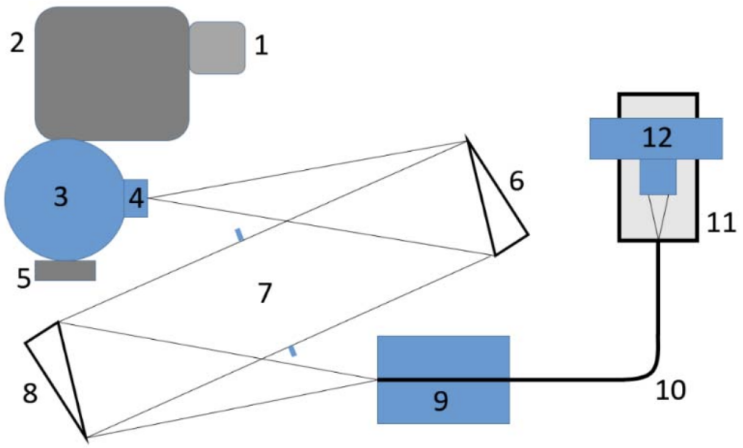

Figure 1: *Schematic for the FRD test.*

The testing setup consists of a laser, a monochromator, photodiode, pinhole, integrating sphere, movement stages, two testing optic fibers, and two shutters. Light passes from the laser through the monochromator (which allows for characterization across various wavelengths) to a beam splitter that splits the light into two paths containing a variety of optical components that allow us to gather data for a given test. A pinhole placed in front of one of the sphere's exit ports ensures uniformity of the illumination. The pinhole is then reimaged by a pair of off-axis parabolas. In the collimated space between the parabolas, an adjustable aperture allows for the $f/\#$ of the fiber injection beam to be varied. By using reflective optics, the need to adjust focus for each wavelength is eliminated, while off-axis parabolas remove the need for a small on-axis fold mirror to avoid vignetting the beam. Moreover, this setup can also accommodate masks that mimic the central obstruction of the telescope, further improving its flexibility and applicability as seen with its utilization for the transmission test.

2.2 Relative Transmission vs Wavelength

The relative transmission of fibers with respect to wavelength is another key characteristic that will determine the overall success of a given test. It refers to the measurement of how efficiently light is transmitted through an optical fiber over different wavelengths of light. Relative transmission is defined as the ratio of the transmitted power to the input power at a specific wave-

length. The transmission of light through an optical fiber depends on the properties of the fiber and the light itself. Different wavelengths of light can interact differently with the fiber material and can have varying degrees of scattering and absorption. As a result, the relative transmission of an optical fiber can vary significantly over different wavelengths.

Measuring relative transmission vs. wavelength is important in characterizing the performance of an optical fiber and determining its suitability for specific applications. For example, in astronomical spectroscopy, the relative transmission of an optical fiber can affect the accuracy of the measured spectral lines, and selecting a fiber with high relative transmission over the desired wavelength range is crucial. For any given instrument, it is imperative that we are able to allow the maximum amount of light to pass through the fibers to reach the instrument it is connected to. Insufficient light will lead to a loss in signal strength and as a result, leads to inaccurate data. In FOCUSS, we will analyze a fiber's ability to sustain high transmission over a range of wavelengths and use that information to categorize them for projects that they are best suited for.

The relative transmission of optical fibers can be measured using the fiber light injection system shown in **Figure 1**. A pinhole with the same diameter as the test fiber is placed at the output of the light injection system, and far-field images of the input spot are taken. The pinhole is then replaced with the test fiber and similar images are taken of the output of the fiber. To ensure that any variations in the light source intensity between the measurements are accounted for, the intensity is measured at a second output port of the integrating sphere that feeds the fiber injection optics. Integration times are adjusted to enable appropriate signal-to-noise of this measurement, so that the overall system throughput requirements of the spectroscopic instrument are met, and systematic errors due to minor throughput variations between fibers can be corrected. The schematic and the lab setup for testing are shown below in **Figure 2**.

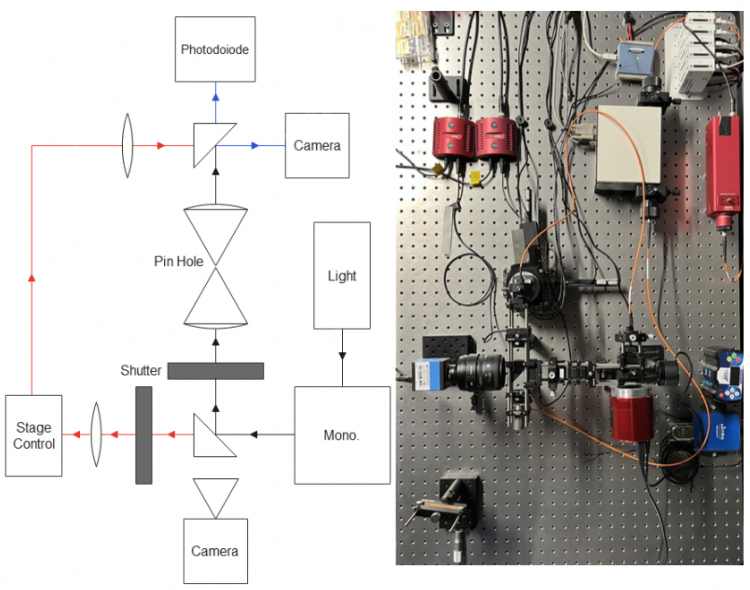

Figure 2: *Schematic and lab setup for Transmission Test.*

2.3 Other characteristics

While the two characteristics listed above are the ones that are primarily looked at, research on other characteristics will be done in tandem, given that there is some overlap among the different tests. These characteristics include:

Flexure Impact: FRD is sensitive to the stress and strain of fibers. The fibers can be manipulated by a robotic stage control in a manner that helps to evaluate these effects on the FRD. In particular, it would shed light on how the FRD will be affected by combinations of bends and twists. This would allow us to find the optimal fiber path for spectroscopic facilities.

Fiber Shape and Scrambling: Groups of fibers that take different paths to a spectrograph experience different bends and levels of strain, which causes inconsistent spectrograph line spread functions. Solutions to fiber scrambling would help produce more stable output and better sky subtraction.

2.4 Automation Algorithms

Large spectroscopic facilities and fiber-fed instruments require thousands of fibers to be characterized, and thus need efficient and consistent testing methods to evaluate them. As such, frequent tasks will be completely automated to streamline the entire process. This includes the automation of the hardware components, such as the operation of the camera, the mechanical shutters, and the rotational stage used to move the fiber. Additionally, it also involves the automation of the data collection process as well. Few of the algorithms used in FOCUSS are described below:

2.4.1 Hill-Climbing Algorithm

The hill-climbing algorithm is an optimization technique used to find the maximum of a function by iteratively making small adjustments to the input values. It is based on the idea of climbing a hill, where each adjustment to the input values represents a step up the hill. The basic principle of hill climbing algorithm is to evaluate all possible neighboring solutions and select the best one to continue the search. The algorithm starts with an initial guess for the input values and then repeatedly makes small adjustments to these values to see if the function value increases. If the function value increases, the new input values are retained and the process continues in the new direction. If the function value does not improve, the algorithm stops and returns the current input values as the local maximum of the function. This process is repeated until a satisfactory solution is found or a stopping criterion is met. It is very efficient for finding local extrema and requires minimal memory and computational resources. In FOCUSS, it is used to control the 6-axis robotic stage control, with the goal of finding the optimal position where the amount of light passing through the fiber is at a maximum. Its implementation is shown below in **Figure 3**.

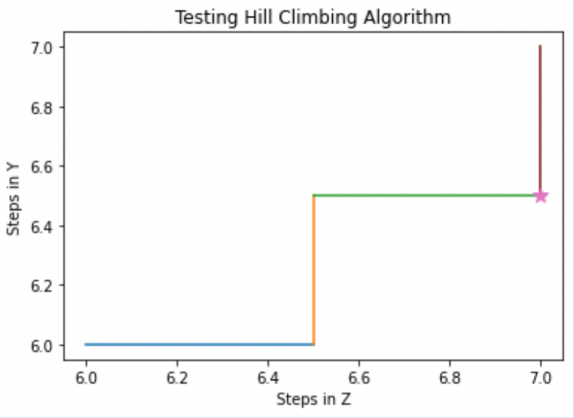

Figure 3: *Visual Representation of steps taken in the Hill Climbing algorithm for the Y and Z axis.*

2.4.2 Ring Test

The ring test is a commonly used technique to determine the presence and severity of the FRD in fiber-fed spectrographs. The test consists of passing light through the fiber and then projecting the light onto a camera. This light detected by the camera appears as "rings", as the name suggests. The beam from the light source is first coupled into the fiber, which then passes through the monochromator that sets it at a particular wavelength. The monochromator then transmits the light to the output end of the fiber. A lens system located at the output end of the fiber then collimates the light and projects it onto a camera or imaging sensor, typically with a long exposure time to capture the faint rings.

The projected rings appear as a series of bright and dark concentric circles on the camera or sensor, with their radii determined by the position of the light on the fiber. Any asymmetry or distortion in the rings is indicative of the presence of focal ratio degradation in the system, which can be quantified by analyzing the shape and intensity of the rings, namely the Full-Width at Half Maximum (FWHM) of the ring.

2.4.2.1 Fiber System Alignment

In order for the above tests to produce accurate results, we first need to align the system in a manner where light passes through the system at maximum intensity. Our Fiber Alignment Script utilizes the hill-climbing algorithm to find the optimal spot for positioning the fiber for the light to pass through. It then sweeps across the full range of each axis of the motor in an increment of 10mm, recording every value measured at each position. At the end of the test, it plots the above values and marks the position where the highest value was detected on the graph. Furthermore, we also fitted a cubic spline to each plot to detect the absolute maximum value and in the process avoid detecting local minima. The rotational stage control moves in 6 directions, and we ran the fiber alignment test on each axis to find the position at which the maximum value is detected by the photodiode.

In the plots shown below, each axis is defined traditionally:

- The X axis represents horizontal (left and right) motion
- The Y axis represents vertical (up and down) motion
- The Z axis represents forward and backward motion
- The Xr axis represents the horizontal tilting (180 degree) motion
- The Yr axis represents the vertical tilting (180 degree) motion

Figure 4 shows the positions that we found for our setup to be the most optimal from the full-range sweep.

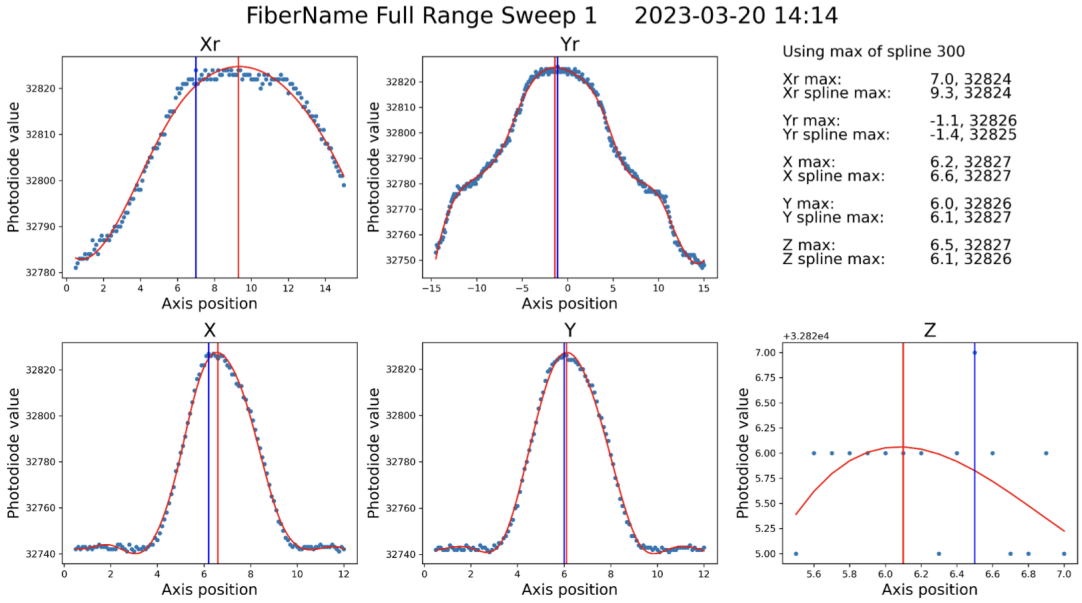

Figure 4: *Results of the Full-Range Sweep for all the axes.*

To ensure the repeatability of these tests, we then implemented a 'finer' sweep that then sweeps over a narrower range of values based off the position where the maximum value was initially detected. The results of the 'finer' sweep are shown below in **Figure 5**.

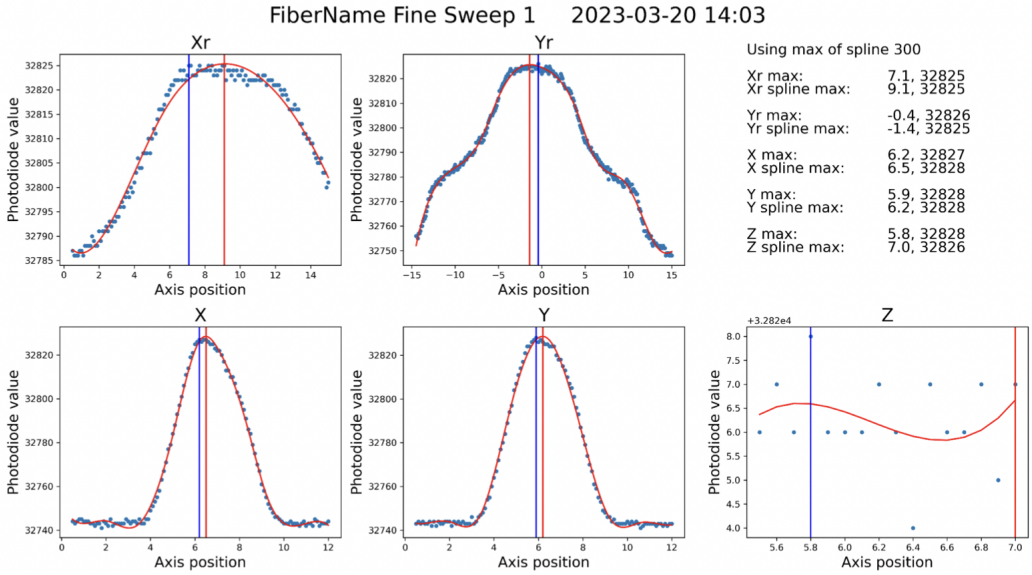

Figure 5: *Results of the Finer Sweep for all the axes.*

It is easily discernible from the above figures that the results produced by the full-range and 'finer' sweep tests are almost identical, and that the fitted cubic spline detects the peaks very well. We can also see that alignment for the Z axis seems to have a lot of variation. However, the Z axis is the axis that moves the fiber forward and backward from the light source, i.e. the highest detected value will be when the fiber is closest to the source. This is clearly seen in the plot for Z axis alignment. Thus, we know that the test was executed well and is fundamentally sound.

2.4.2.2 FRD Image Analysis

The image analysis technique used in FOCUSS is used to determine the FWHM and the FRD of the ring-like image that the fiber produces when the light passes though it. This is done by first initializing rotation angles for the input image. Due to the presence of background and systematic noise in the raw data, the processing and analysis of such data can be challenging. In order to mitigate the impact of these noise sources, a smoothing step is often performed to improve

the signal-to-noise ratio. In our algorithm, a 1D Box filter kernel (convolution kernel) is used to smooth the data. Next, the algorithm divides the data into different segments based on the amount of noise in the raw data. The mean intensity of the data in each segment is then calculated, and the data is subsequently interpolated based on these mean values. This smoothing step enables the identification of important features and patterns in the data, which would otherwise be obscured by the presence of noise.

The script proceeds with the analysis of the projected ring image only if there are well-defined contours after smoothing out the noise. The absence of clear peaks negatively impact the FRD calculation. The code looks for images where the light is scattered azimuthally instead of radially, ensuring a more uniform ring. A comparison of a ring image with well-defined contours vs an image without well-defined contours is shown below in **Figure 6**.

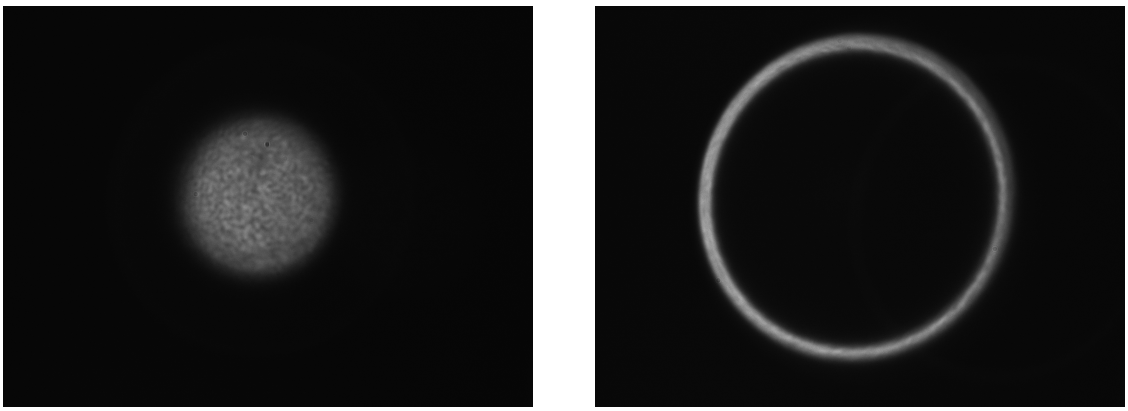

Figure 6: *Image of a projected ring without defined contours(left) vs image of a projected ring with well-defined contours (right).*

We smooth over the data 4 times to ensure that there is no extraneous background noise. The refined image is then used to calculate the center of the ring, with the help of the OpenCV package. OpenCV is a widely-used computer vision library that provides a range of tools for image and video processing. The package includes functions for image filtering, feature detection, and object recognition. The functions provided by OpenCV are used to apply Gaussian blurring

and thresholding to the input image, locate the contour of the circle, and its FWHM.

The FWHM is calculated by using cubic spline interpolation to find the roots of the difference between the y values and the half-maximum of the y values corresponding to those within the contour and close to the center of the ring. The distance between the two roots is returned as the FWHM, along with the two roots that specify the center. Using these coordinates, the image is then rotated by each of the angles specified. A slice of the rotated image is then taken along the Y axis passing through the center of the circle, and the FWHM function is applied to the slice. The resulting FWHM is then averaged over all the rotations to obtain a smoothed curve of the FRD.

The smoothed curve is then plotted, and the peaks are identified. The diameter of the circle is then calculated as the distance between the first two peaks. The smoothed curve is split in half, and the FWHM function is applied to each half to calculate the FWHM for each respective half. The difference in the x-coordinates of the two roots of the difference between the two halves is taken as the FRD, which is then plotted along with the smoothed curve of the degradation. An example of the individual plots produced at each degree can be seen below in **Figure 7**, which shows the image analysis for a particular angle at a particular wavelength. The remaining subplots can be found in **Appendix A: Plots**.

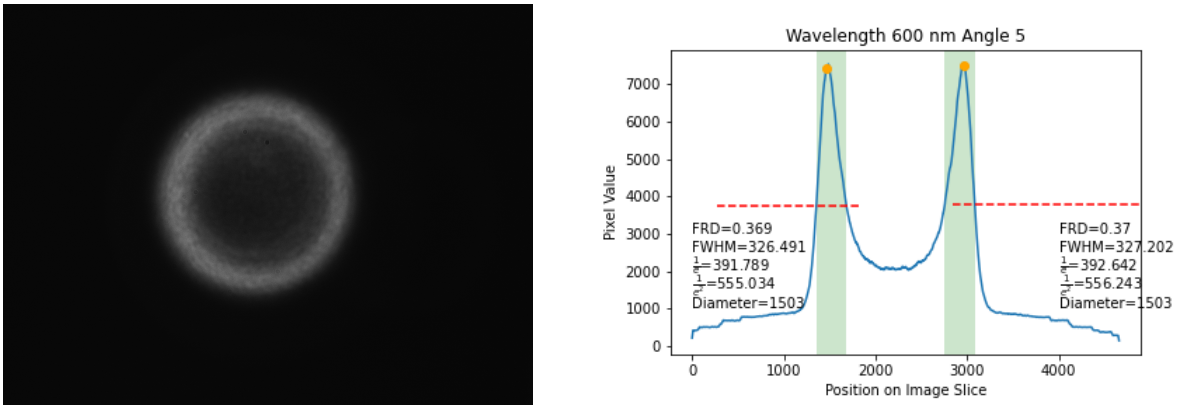

Figure 7: *Image of projected ring at a wavelength of 600nm at 5deg (left) with its corresponding image analysis (right).*

The end result of this application produces a graph that shows how the FRD varies with the angle at which fiber is tilted. This is shown in the Results section.

2.4.3 Transmission Test

The Transmission Test is a script that will analyze and plot the data used to determine the relative transmission vs wavelength. The test consists of using two shutters to alternate between measuring the intensity of the light passing through a reference path (which simulates perfect transmission) and a sample path (which simulates blocked transmission). The ratio of the two measurements provides the relative transmission of the sample at each wavelength. Similar to the FRD test, we use the Fiber Alignment Algorithm to align the system, as well as the monochromator to set the beam of light to the respective wavelengths.

3. RESULTS

The preliminary results of the Ring test and the Transmission Test are presented in the section below.

3.1 Ring Test

Using the collected data, we averaged the range of motion of the robotic axis, and created an averaged graph of the output for the tests. The plot of the FRD vs the incident angles at a wavelength of 600nm is shown in **Figure 8**.

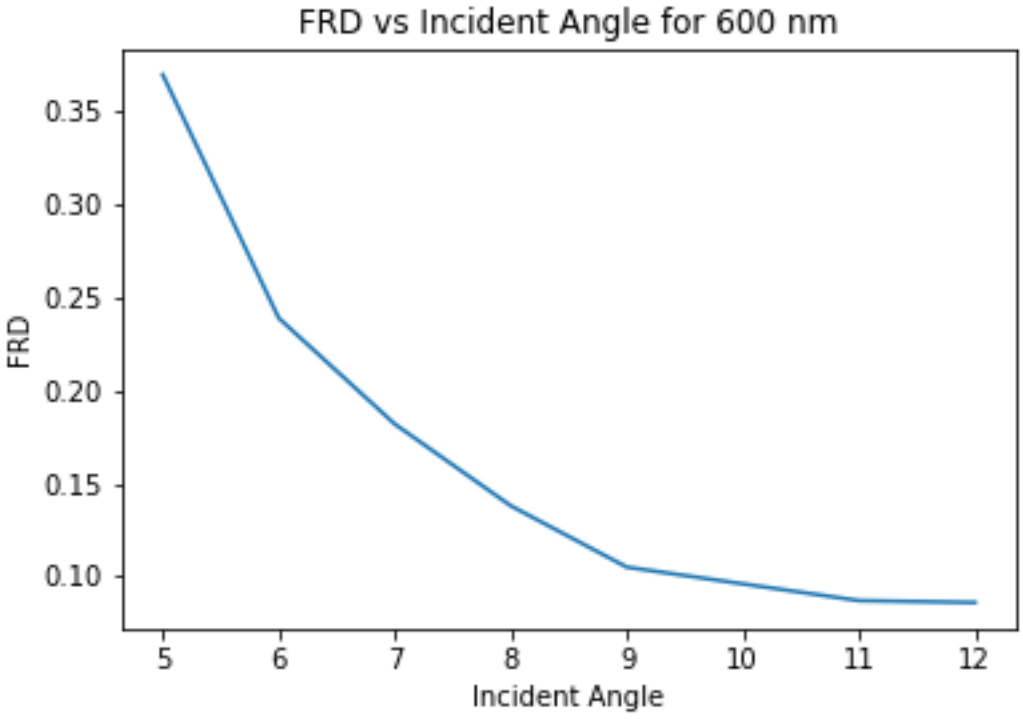

Figure 8: *FRD vs input angle plot at 600 nm.*

As seen above, the FRD has a range of angles where its effects are minimized. Extremely

low angles produce a higher FRD. This is due to the fact that at low angles, the amount of light that passes through the fiber is drastically lower than when it is in line with the light source. The FRD was at its lowest when the wavelengths are at the visual band, and when the injection angles were higher (from 10-12 degrees).

As part of the analysis, we calculated some intermediate values necessary to calculate the FRD. This includes the $1/e^2$ value, which is when the system has 13.5% of the peak intensity. The $1/e^2$ value is derived by converting the FWHM calculated during the analysis. We also calculate the diameter of the projected ring. From the calculated $1/e^2$ and the diameter values, we were able to calculate the FRD using the formula below:

$$\mathbf{FRD} = \frac{1/e^2}{D} \tag{1}$$

We were also able to determine the $f/\#$ for the fiber using the calculated values above. The ideal $f/\#$ for a fiber injection system depends on various factors, such as the numerical aperture of the fiber and the size of the telescope beam. In general, a smaller $f/\#$ allows for more efficient coupling of light into the fiber, but may also result in a higher FRD due to a larger cone angle. On the other hand, a larger $f/\#$ may result in less FRD but also less efficient coupling of light into the fiber. The optimal $f/\#$ is therefore a trade-off between these factors and is typically determined empirically for a given telescope and fiber system. For the test fiber that we used, we have found that our lowest FRD of 7% was found at $f/3$.

Overall, the results that we have attained are very encouraging. Shown below in **Figure 9** is a comparison of our results with that of Monty et.al. [13]. They also use a fiber testing bench with an apparatus very similar to the one used for FOCUSS, along with the accompanying procedures to automate the system. Note that we focus on positive angles while [13] has repeated the test for negative angles as well.

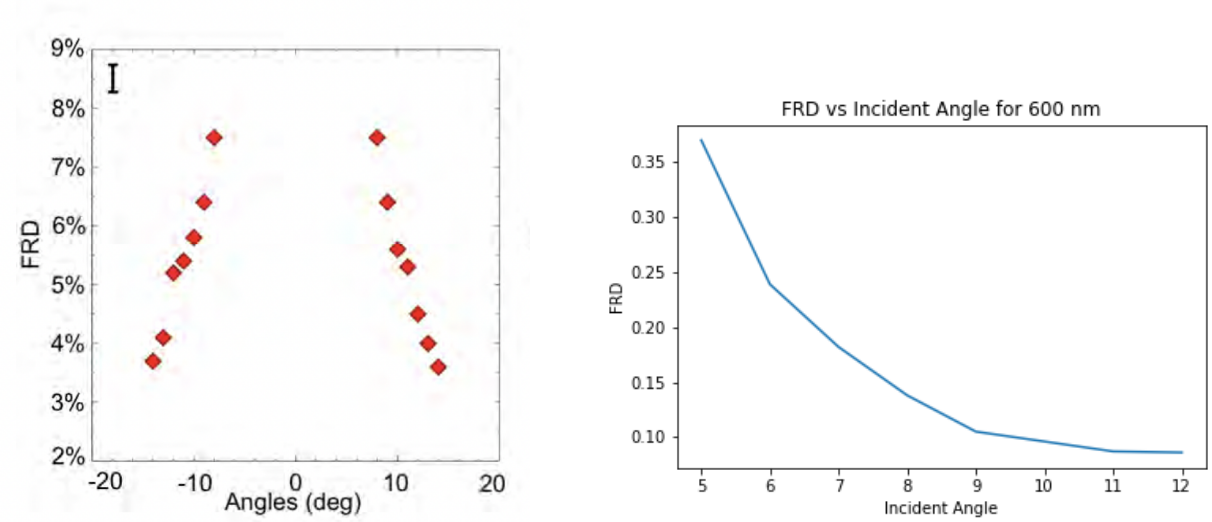

Figure 9: *FRD analysis by [13] (left) compared to our FRD analysis (right).*

As seen above, the FRD plot that we produced shows that the behavior of the fiber is the same as that done by [13], where the FRD decreases as the incident angle is increased. While our results are not as accurate, this was the first iteration of our test, and shows that the project is heading in the right direction, and that the scripted tests are working as expected.

Several strategies can be employed in order to reduce the impact of FRD on fiber optic systems. First, using high-quality, low-stress fiber with a controlled core diameter and numerical aperture can help reduce FRD caused by fiber imperfections. Second, improved connector design can be utilized by using connectors with low insertion loss and a carefully designed interface to reduce the amount of light scattered at the connector and improve the efficiency of coupling light into the fiber. Additionally, reducing fiber bending by avoiding sharp bends in the fiber and minimizing the length of fiber that is bent can decrease the amount of light scattered due to microbending and improve the efficiency of coupling light into the fiber. However, large spectroscopic facilites have upwards of 30,000 fibers per instrument so it could be difficult managing them. Minimizing fiber movement during use, such as by securing it in place, can also reduce the amount of light scattered due to macrobending and improve the efficiency of coupling light into the fiber. Finally, active feedback control can be implemented to maintain a constant coupling efficiency between the fiber

and the source, which can reduce the impact of FRD on the overall system performance. We will be implementing these suggestions gradually as the project progresses.

3.2 Transmission Test

We ran the test over a series of wavelengths ranging from 500 nm in the visual spectrum to 750 nm in the near-infrared spectrum. As mentioned earlier, the shutters alternated through the reference path and the blocked path for each wavelength, increasing in 1 nm intervals. Ten data points were collected at each shutter state and then averaged to produce the resulting photodiode value for that single state. After the test has sweeped through the entire wavelength range, the averaged dark state values are subtracted from the "imperfect" transmission state values, and then averaged with the "perfect" transmission values for each wavelength respectively. The result of one iteration of the transmission test is shown below in **Figure 10**.

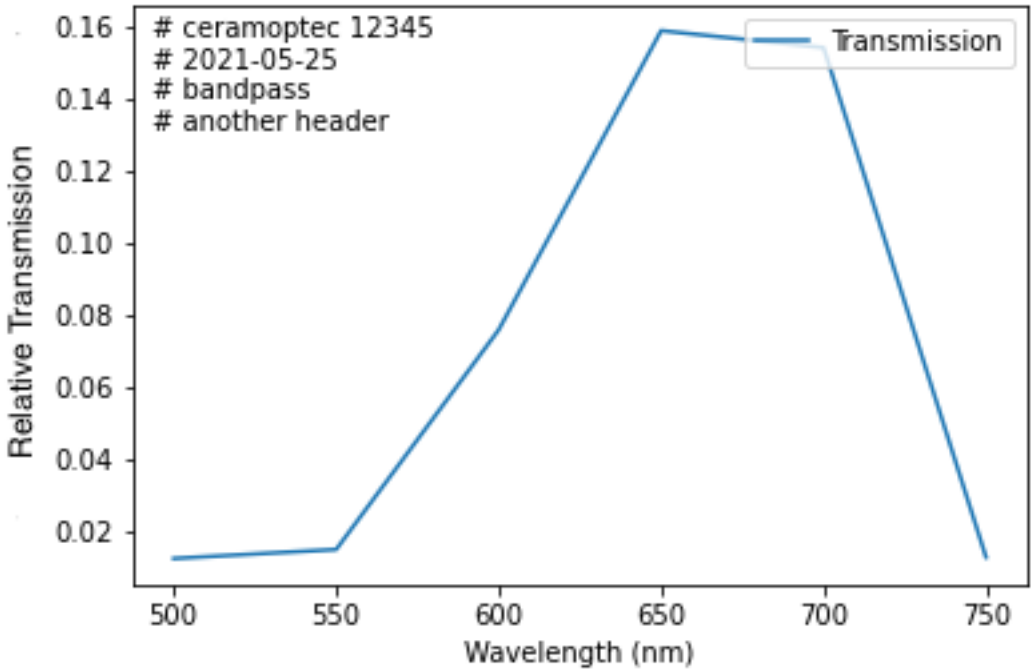

Figure 10: *Relative Transmission vs wavelength plot for the test fiber.*

We can see that the transmission peaks for the wavelength range of 650nm to 710nm, right in the middle of the visual band. However, we can also see that the peak transmission attained is capped at 16%, an uncharacteristically low value. We think that the pinhole we used in the apparatus was faulty, resulting in the fiber having a higher transmission compared to the "perfect transmission" that the pinhole was supposed to simulate. This resulted in a very low ratio between the two transmission states and subsequently led to a low relative transmission. A example plot of the data that we would ideally expect to produce is shown below in **Figure 11**.

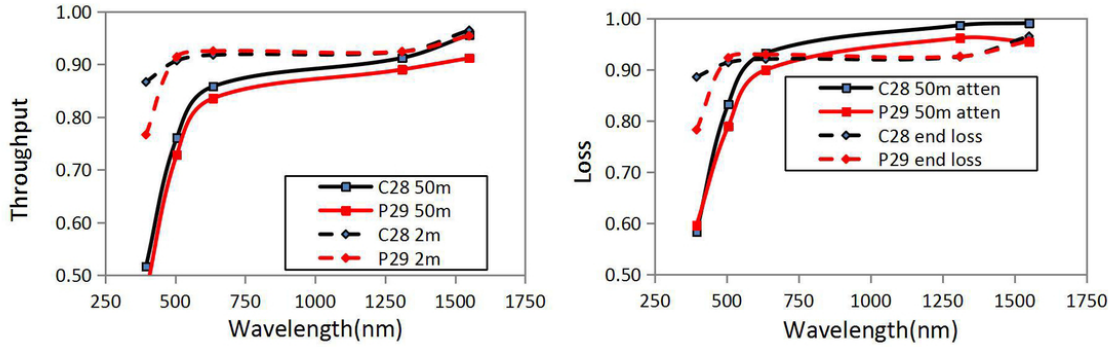

Figure 11: *Sample Relative Transmission vs Wavelength Plot.[14]*

The plot was produced by [14] in an effort to measure fiber performance for a set of high numerical aperture fibers. As part of their study, they tested the FRD and throughput of the fibers, as well as compared their attenuation losses to the best available standard fibers that are considered to be "high-performance fibers". For the fibers that they tested (dotted lines), the peak transmission is around 95%, and is no lower than 75% as seen in the figure above. These are the kind of results that we expect to produce in the future.

However, low transmission in optical fiber systems can be caused by a variety of other factors, including attenuation, dispersion, reflection, equipment failure, and wavelength dependency. Attenuation can occur due to impurities in the fiber, bending or twisting of the fiber, or splices and connectors between fiber sections. Dispersion can result from variations in the refractive index

of the fiber, which lead to different propagation speeds for different wavelengths. Reflection can occur at splices and connectors or at the interface between the fiber and transmitting or receiving devices. Equipment failure, such as a damaged or misaligned connector, a malfunctioning laser, or a faulty photodiode can also contribute to low transmission. Finally, optical fibers can also exhibit wavelength-dependent losses, leading to variations in transmission efficiency as a function of wavelength. Accurately diagnosing the cause of low transmission requires careful analysis of the transmission spectrum, as well as any relevant data or information about the fiber and associated equipment. By doing so, it is possible to identify and address the root cause of low transmission, and improve the overall performance of the optical system. That will be the next step taken, along with collecting more data at each shutter state.

4. CONCLUSION

4.1 Characteristic Categorization

FOCUSS has allowed us to develop techniques to measure various fiber characteristics relevant to astronomical instrumentation. Through this project, we were able to perform a comprehensive study on two key fiber characteristics - Focal Ratio Degradation (FRD) and Relative Transmission vs Wavelength, and highlight the significance of accurately characterizing these parameters. The development of a fiber-testing suite enabled the testing of these characteristics and the generation of numerous automation algorithms with a wide range of applications. The findings of our project emphasize the importance of accurately characterizing FRD and Relative Transmission in selecting fiber packages for future astronomical facilities. The results obtained from testing these characteristics can aid in the development of improved fiber designs with reduced FRD and increased transmission efficiency. The immediate next steps for the FOCUSS software involve further optimizing the alignment by creating an "offset sweep", which moves the 6-axis robotic stage control to a random position and starts the alignment from there, to ensure that there is no bias stemming from the initial position. With regard to the hardware, we will introduce a different pinhole and collimator to accurately simulate the perfect transmission state. The completion of these steps should set up another run of the FRD and transmission tests. The big-picture applications of FOCUSS are described below.

4.2 Future work

The implementation of the suggestions attained from FOCUSS can be useful to a multitude of projects. The Maunakea Spectroscopic Explorer (MSE) is a massively multiplexed spectroscopy facility[12] that will be the first to implement the findings of FOCUSS. Below are some key projects that cannot be executed with current generation instrumentation, but that greatly benefit from this suite of characteristic categorizations in tandem with the MSE.

Advancing knowledge on the nature of dark matter: By studying the velocities of stars in

stellar streams and dwarf galaxies in the local Universe, as well as gravitationally lensed systems of galaxy clusters in the distant Universe, we can obtain valuable insights into the nature and properties of dark matter halos. In particular, large-scale precision measurements of faint sources enabled by the capabilities of the MSE will provide unprecedented opportunities to accurately determine the properties of dark matter halos, including the dark matter subhalo mass function, and the dark matter halo density profiles [15]. These measurements will enable us to effectively constrain the properties of cold dark matter, and provide us with a means of testing whether it is purely collisionless or not.

Next Generational Cosmological Studies: The measurement of the scale-dependent growth of matter fluctuations can provide crucial insights into the early universe and the fundamental physics that governs its evolution [16]. One key parameter of interest is the summed neutrino mass, which has been predicted by the standard model of particle physics, but has yet to be measured directly. The discovery of neutrino oscillations could indicate that their total mass could have a significant impact on the large-scale structure of the universe. They would also help refine our understanding of the processes that led to the formation of large-scale structure in the universe. The measurement of these parameters requires large-scale surveys of the universe. FOCUSS will help spectroscopic explorers such as the MSE obtain exceedingly clean calibrated data, and when combined with measurements from other surveys at different redshifts, such as DESI and CMBS4, these surveys can enable measurements of both the summed neutrino mass and the hierarchy of masses, as well as provide valuable insights into the physics of inflation and galaxy formation.

Multi-messenger and time domain astronomy: The study of galaxy evolution has been a focal point in astronomy for decades, with significant progress made in understanding the properties of galaxies, including their morphologies, star formation rates, and chemical compositions. However, our current knowledge of galaxy formation and evolution is far from complete, with many unanswered questions remaining, such as the role of dark matter in galaxy formation, the driving mechanisms behind galaxy mergers and starburst events, and the relationship between galaxies and their environments. The MSE will play a crucial role in advancing our understanding of galaxy

evolution by providing high-quality spectroscopic observations of millions of galaxies over a wide range of redshifts. Through its unique capabilities, it will help us address many of the outstanding questions in galaxy formation and evolution, and shed light on the complex relationship between galaxies and their environments [17].

Overall, the FOCUSS project has significantly advanced our understanding of fiber characteristics relevant to astronomical instrumentation and has provided valuable insights into their characterization and selection. The methodologies and techniques developed through this project can be utilized in future fiber characterization studies, enabling continued progress in the field of astronomical instrumentation.

REFERENCES

[1] S. Ellis, W. Saunders, C. Betters, and S. C. 2014, "The problem of scattering in fibre-fed vph spectrographs and possible solutions," *SPIE*, vol. 9151, July 2014.

[2] M. Rodrigues, H. Flores, M. Puech, Y. Yang, and F. Royer, "A method to subtract the skylight for the multi-fiber instrument e-elt/optimos-eve," *SPIE*, vol. 7735, July 2010.

[3] M. Puech, M. Rodrigues, Y. Yang, H. Flores, F. Royer, K. Disseau, T. Gonçalves, F. Hammer, M. Cirasuolo, C. J. Evans, G. L. Causi, R. Maiolino, and C. Melo, "Sky background subtraction with fiber-fed spectrographs," *SPIE*, vol. 9147, July 2014.

[4] M. Puech, H. Flores, Y. Yang, M. Rodrigues, T. Goncalves, F. Hammer, and K. Disseau, "Characterizing the red optical sky background fluctuations from narrow-band imaging," *SPIE*, vol. 8446-292, July 2012.

[5] J. Stover and R. Tuthill, "Focal ratio degradation caused by surface scattering and bulk absorption in mirrors and lenses," *Applied Optics*, vol. 4009-4018, July 1983.

[6] A. Hagen, J. Foo, J. Bland-Hawthorn, and J. Lawrence, "Focal ratio degradation in optical fibers," *Monthly Notices of the Royal Astronomical Society*, vol. 1789-93, no. 1, 2008.

[7] J. Bland-Hawthorn, S. Gondhalekar, D. Lee, J. Martin, and R. Sharples, "The optical design of the fiber-fed integral field unit for virus," *Publications of the Astronomical Society of the Pacific*, vol. 1437-46, no. 889, 2010.

[8] W. Saunders, R. Butler, C. Tinney, and J. Bland-Hawthorn, "Focal ratio degradation by misalignments in fiber-fed spectrographs," *Publications of the Astronomical Society of Australia*, vol. 380-85, no. 4, 2012.

[9] A. Tokovinin, M. Schoeck, and A. Rademacher, "Focal ratio degradation in the gemini-south telescope: observations and model," *Monthly Notices of the Royal Astronomical Society*, vol. 1311-19, no. 2, 2015.

[10] M. Goodwin, D. Gavel, C.Lockwood, and K. Powell, "A method for measuring focal ratio degradation using a pinhole camera," *Publications of the Astronomical Society of the Pacific*, vol. 045002, no. 998, 2018.

[11] J. D. Murphy, P. J. MacQueen, G. J. Hill, F. Grupp, A. Kelz, P. Palunas, M. Roth, and A. Fry, "Focal ratio degradation and transmission in virus-p optical fibers," *SPIE*, vol. 7018, no. 10, 2008.

[12] J. L. Marshall, "Ati proposal," *NSF*, 2019.

[13] S. Monty, F. Jahandar, J. Lee, K. A. Venn, C. Bradley, D. Erickson, D. Crampton, V. Nicolov, C. L. Kielty, C. Mazoukh, and P. Hall, "Automated testing of optical fibres: towards the design of the maunakea spectroscopic explorer fibre transmission system," *SPIE*, 2018.

[14] K. Zhang, J. R. Zheng, and W. Saunders, "High numerical aperture multimode fibers for prime focus use," *SPIE*, 2016.

[15] T. Li and M. Kaplinghat, "Dark matter physics with wide field spectroscopic surveys," *Astro2020 Decadal Survey*, 2019.

[16] W. Percival and C. Yeche, "Cosmology with the maunakea spectroscopic explorer," *MSE Science Case*, 2019.

[17] Y. Shen, "Mapping the inner structure of quasars with time-domain spectroscopy," *Astro2020 Decadal Survey*, 2018.

APPENDIX A: PLOTS

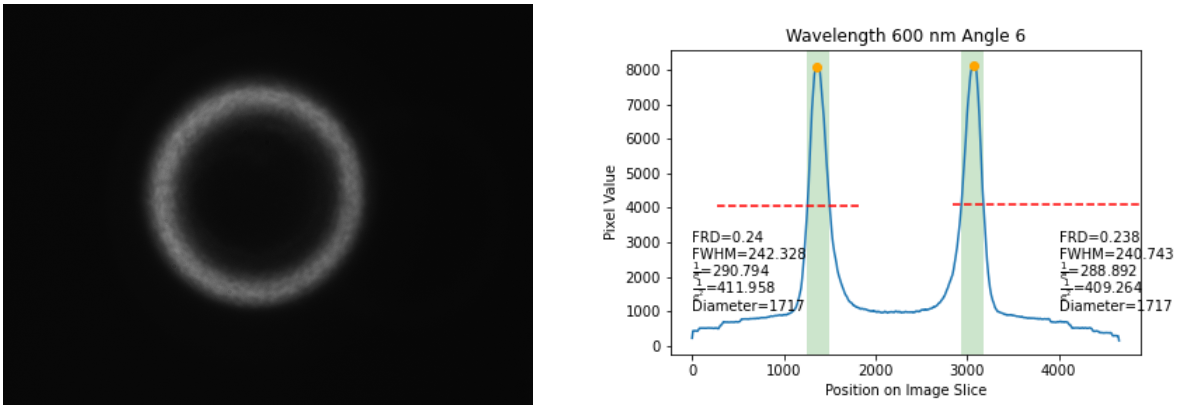

Figure A.1: *Image of projected ring at a wavelength of 600nm at 6deg (left) with its corresponding image analysis (right).*

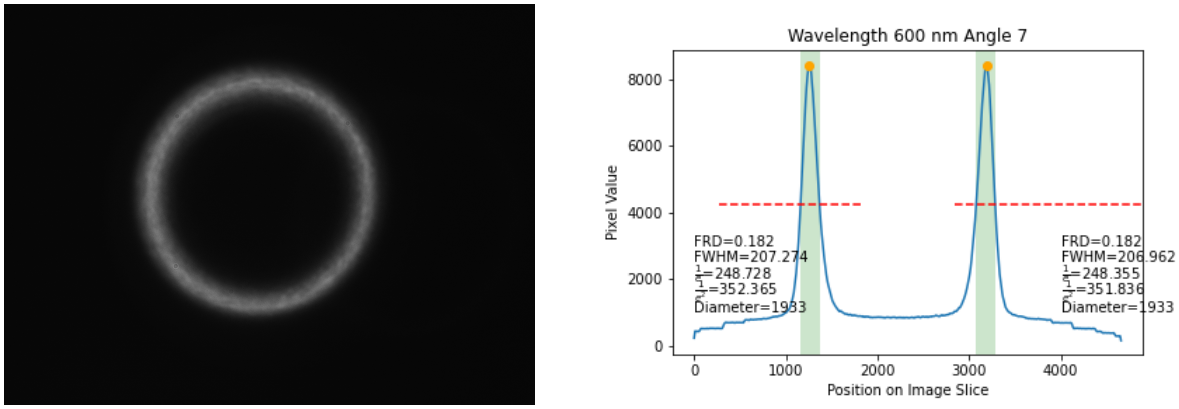

Figure A.2: *Image of projected ring at a wavelength of 600nm at 7deg (left) with its corresponding image analysis (right).*

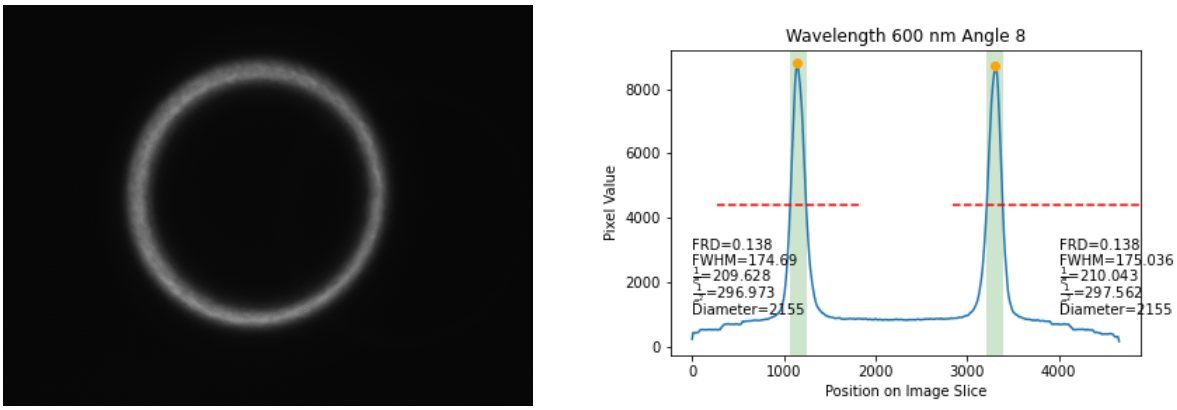

Figure A.3: *Image of projected ring at a wavelength of 600nm at 8deg (left) with its corresponding image analysis (right).*

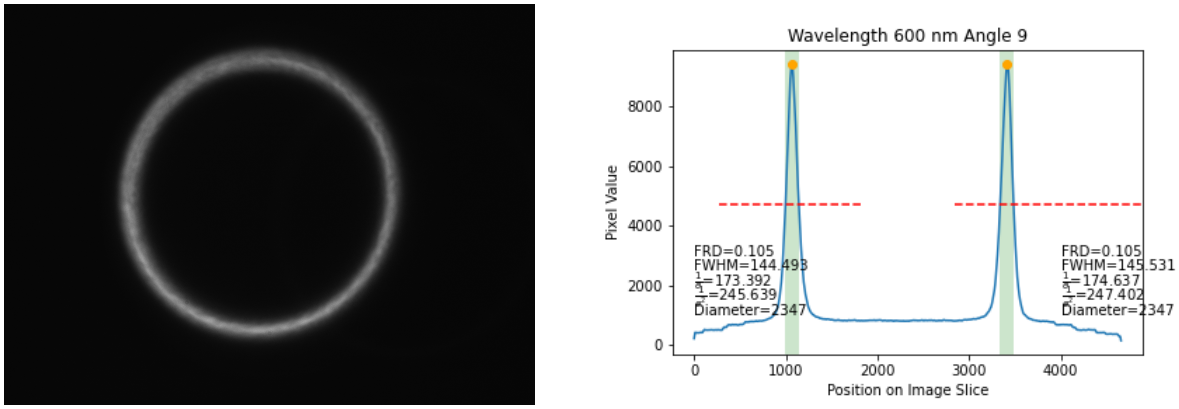

Figure A.4: *Image of projected ring at a wavelength of 600nm at 9deg (left) with its corresponding image analysis (right).*

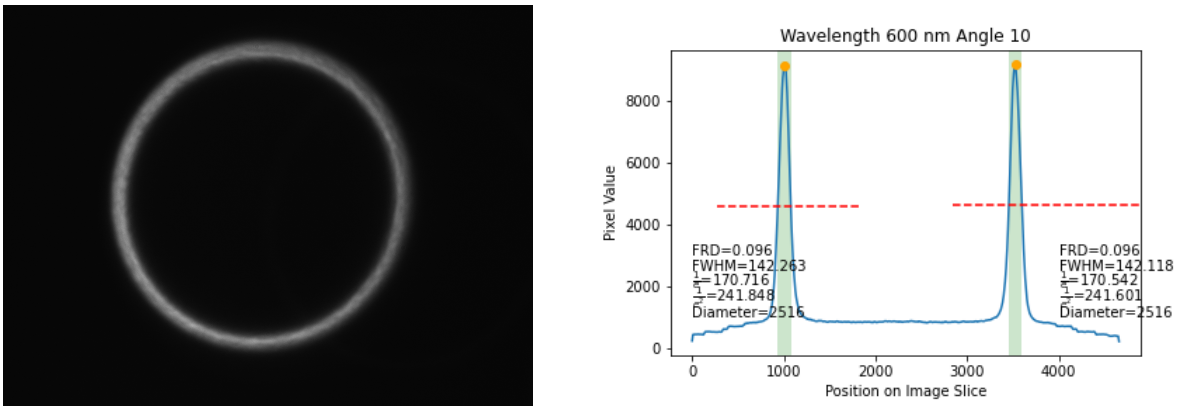

Figure A.5: *Image of projected ring at a wavelength of 600nm at 10deg (left) with its corresponding image analysis (right).*

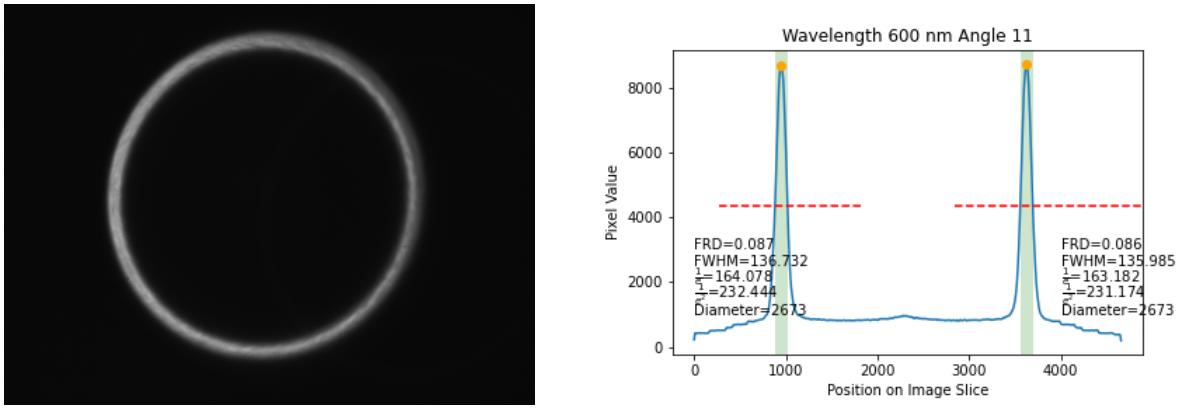

Figure A.6: *Image of projected ring at a wavelength of 600nm at 11deg (left) with its corresponding image analysis (right).*

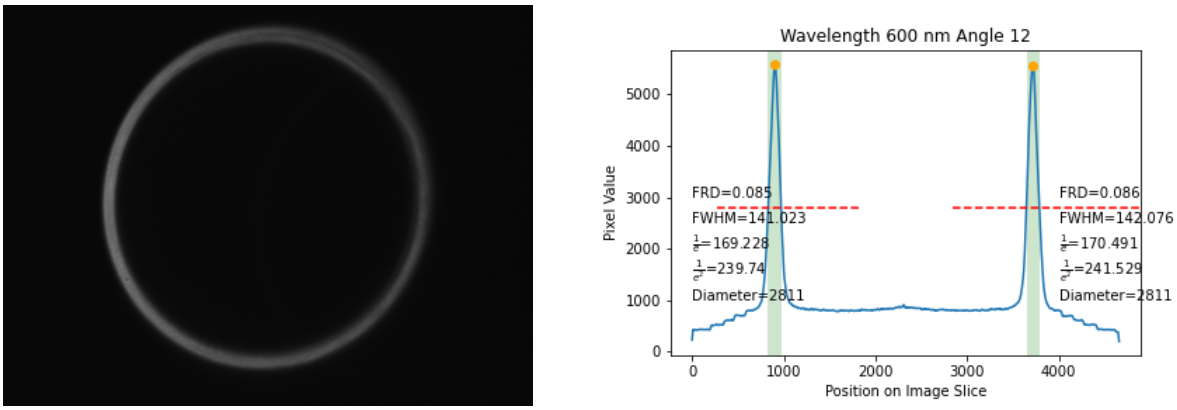

Figure A.7: *Image of projected ring at a wavelength of 600nm at 12deg (left) with its corresponding image analysis (right).*